EQA - International Journal of Environmental Quality
ISSN 2281-4485 - Vol. 75 (2026): 62 - 73
Journal homepage: https://eqa.unibo.it/

published by

Associations of vegetation, microbial communities, and soil properties with mineral-associated organic carbon in karst soils

Hefeng Wan [1,2*], Lei Hao [1,2], Xiuyuan Yang [1,2], Jing Wang [1], Guohua Liu [1], Jiang Hong [3]

[1] Guizhou Institute of Biology, Guizhou Academy of Sciences, Guiyang, Guizhou, China
[2] Fanjing Mountain Forest Eco-station, Guizhou Institute of Biology, Jiangkou, Guizhou, China
[3] Guizhou Academy of Sciences, Guiyang, Guizhou, China

* Corresponding author E.mail: whefeng@126.com

Article info
Received 13/5/2026; received in revised form 19/8/2026; accepted 5/9/2026
DOI: 10.60923/issn.2281-4485/25018

Abstract
Mineral-associated organic carbon (MAOC) is an important component of stable soil carbon pools, yet its distribution and controlling factors in karst ecosystems remain unclear due to strong soil heterogeneity. This study investigated the relationships between vegetation type, microbial communities, soil physicochemical properties, and MAOC amount in a karst watershed in Guizhou, China. Surface soils (0–20 cm) were collected from limestone-derived Leptosols under three vegetation types: grassland, arboreal forest, and shrubland. Soil physicochemical properties were analyzed in combination with high-throughput sequencing of bacterial 16S rRNA genes and fungal ITS regions. MAOC content was highest in arboreal forest soils (5.54 g/kg), followed by shrubland (2.83 g/kg) and grassland (1.84 g/kg). Microbial richness and diversity did not differ significantly among vegetation types, although bacterial diversity was consistently higher than that of fungi. Dominant bacterial phyla included Proteobacteria, Acidobacteriota, and Actinobacteriota, while fungal communities were dominated by Ascomycota, with relatively higher abundances of Basidiomycota and Rozellomycota in arboreal forest soils. Soil chemical properties showed no significant differences among vegetation types, whereas soil texture varied significantly. Across the study area, MAOC was positively associated with Actinobacteriota abundance, soil pH, and sand content, and negatively associated with clay and silt contents. These findings indicate that MAOC variation in karst soils is closely associated with vegetation type, soil texture, and microbial community composition. Arboreal forest soils were associated with relatively higher MAOC levels, highlighting the importance of vegetation–soil–microbe interactions in soil carbon stabilization and ecosystem quality in carbonate landscapes.
Keywords: *mineral-associated organic carbon · karst soils · microbial community · soil texture · carbon stabilization*

Introduction

The stabilization of soil organic carbon (SOC) is an important process for maintaining soil quality, ecosystem functioning, and climate change mitigation. Mineral-associated organic carbon (MAOC) represents a relatively stable SOC fraction because organic compounds can be protected through ligand exchange, cation bridging, mineral adsorption, and co-precipitation at mineral interfaces (Sokol *et al.* 2022; Georgiou *et al.* 2024; Tong *et al.* 2024). Globally, MAOC may account for a large proportion of SOC storage, but its contribution varies greatly among ecosystems because of differences in soil texture, mineral composition, pH, hydrology, nutrient availability, and carbon inputs (Lv *et al.* 2023; Georgiou *et al.* 2022; Zhou *et al.* 2024). Chemical bonding and physical protection are generally considered two major mechanisms of MAOC stabilization. The former includes interactions between organic functional groups and mineral surfaces, such as carboxyl–Fe^{3+} ligand exchange and Ca^{2+}-mediated bridging, whereas the latter involves multilayer adsorption and mineral co-precipitation that reduce organic carbon decompo-

EQA 75 (2026): 62 - 73

DOI: 10.60923/issn.2281-4485/25018

sition (Underwood *et al.* 2024; Tong *et al.* 2024). However, the relative importance of these processes is environmentally dependent. In neutral to alkaline carbonate soils, calcium-mediated interactions may be particularly important for the formation and persistence of organo-mineral associations (Bi *et al.* 2024; Underwood *et al.* 2024). Microorganisms play a central role in SOC transformation and MAOC formation. Through metabolic processing, bacteria and fungi decompose plant residues and produce low-molecular-weight organic compounds, extracellular polymeric substances, and microbial residues that can interact with mineral surfaces (Angst *et al.* 2021; Zhu *et al.* 2024). Fungal hyphae, bacterial cell-wall residues, and microbial necromass may contribute to stable carbon pools through mineral adsorption, Ca^{2+} bridging, and physical protection within soil aggregates, which limits microbial decomposition (Song *et al.* 2023; Su *et al.* 2024). At the same time, microbial effects on MAOC are regulated by soil properties, nutrient stoichiometry, substrate availability, and microbial carbon use efficiency (Li *et al.* 2024b; Wu *et al.* 2025). Therefore, microbial diversity alone may not fully explain MAOC amount. The composition of specific microbial groups and their relationships with soil physicochemical conditions may provide more useful indicators of soil carbon stabilization and soil ecosystem quality. Karst ecosystems provide a special context for studying MAOC because they are characterized by shallow soils, exposed carbonate bedrock, rapid hydrological exchange, and fragmented vegetation cover (Li *et al.* 2025a; Xiao *et al.* 2025). These features may restrict soil development and reduce continuous organo-mineral contact, while carbonate weathering and high Ca^{2+} availability may enhance calcium-mediated stabilization pathways (Bi *et al.* 2024; He *et al.* 2024). As a result, MAOC dynamics in karst soils may differ from those in non-carbonate systems. For example, clay-rich soils are commonly expected to favor SOC stabilization, but this relationship may be weakened or even altered in carbonate soils if Ca-mediated interactions, drainage conditions, or microbial substrate limitation become more important than clay-controlled adsorption (Hu *et al.* 2024; Zhou *et al.* 2024). Such complexity makes karst soils highly suitable for examining how vegetation, microbial communities, and soil properties jointly relate to MAOC amount. Vegetation cover can influence MAOC through differences in litter input, root activity, nutrient cycling, soil microclimate, and microbial community composition. Forest, shrubland, and grassland soils often differ in organic matter inputs and microbial habitats, which may lead to different patterns of SOC stabilization (Liao *et al.* 2023; Liang *et al.* 2023). However, in karst landscapes, these vegetation effects are likely to interact with strong soil heterogeneity and possible land-use legacy. Because MAOC usually has a relatively long turnover time,observed vegetation–MAOC relationships should be interpreted cautiously as associations rather than direct causal effects unless they are supported by experimental evidence. This is particularly important in heterogeneous carbonate soils, where current vegetation patterns may reflect both present-day plant inputs and historical changes in soil properties and microbial communities. In this study, we investigated MAOC amount under three vegetation types, namely grassland, arboreal forest, and shrubland, in a small karst watershed on the Guizhou Plateau (Dai *et al.* 2023). By combining soil physicochemical measurements, soil texture analysis, nutrient stoichiometry, and high-throughput sequencing of bacterial 16S rRNA genes and fungal ITS regions, we aimed to examine: (1) how MAOC content varies among vegetation types in limestone-derived karst soils; (2) which soil physicochemical properties and microbial groups are associated with MAOC variation; and (3) whether these associations indicate vegetation-specific patterns of carbon stabilization in heterogeneous carbonate soils. We hypothesized that MAOC variation would be closely associated with vegetation-related differences in microbial community composition and soil physicochemical properties, especially soil texture, pH, and nutrient stoichiometry.

Materials and methods

Study area overview

The study area is located in Puding County, Anshun, Guizhou Province, a representative karst region in central Guizhou, China. Karst landscapes account for approximately 84.26% of the total land area and are characterized by complex geomorphology, diverse landforms, and strong spatial heterogeneity. The ecosystem is considered fragile and has been affected by long-term human disturbance, including agricultural expansion, vegetation degradation, and rocky desertification (Bi *et al.* 2024; Zhang 2017). However, relatively undisturbed vegetation patches remain, providing suitable conditions for comparing vegetation–soil carbon relationships within a consistent watershed context. The region has a subtropical humid monsoon

DOI: 10.60923/issn.2281-4485/25018

climate, with a mean annual precipitation of 1,378.2 mm, mean annual temperature of 15.1°C, and average annual sunshine duration of 1,164.9 h (Zhang 2017; Bi *et al.* 2024). Elevation ranges from approximately 1,200 to 1,500 m based on 30 m resolution DEM data, with the central Chengguan River watershed located at relatively lower elevations (Bi *et al.* 2024). Sampling sites were distributed within the Chengguan River watershed (Fig. 1), and detailed vegetation characteristics are provided in Appendix A.

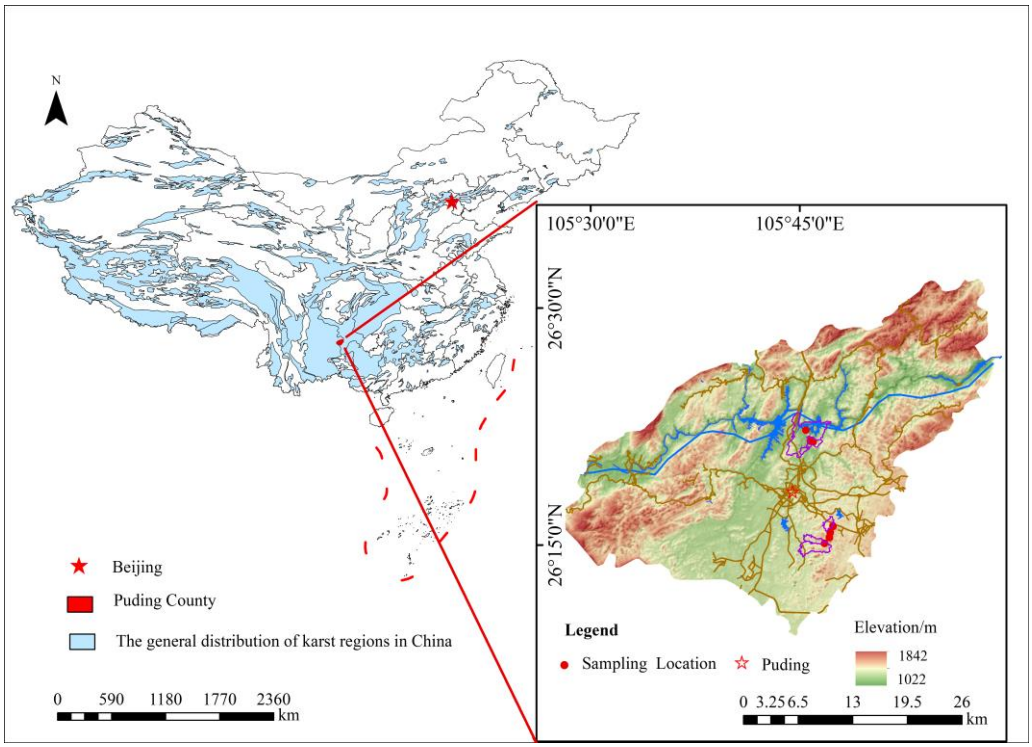

Figure1
Distribution map of the location and soil sample location.

Sample collection and soil analysis

To reduce spatial variability, sampling sites were selected under comparable topographic conditions, similar parent material, and relatively consistent vegetation structure. All sites were located on mid-slope positions, avoiding ridge and valley-bottom microhabitats. Sampling areas were restricted to soils developed from limestone parent material with relatively low bedrock exposure (< 30%), thereby minimizing lithological and structural heterogeneity (Bi *et al.* 2024). Soil samples were collected from the surface layer (0–20 cm) of limestone-derived Leptosols. This depth was selected to represent the main zone of plant–soil–microbe interactions and to ensure comparability across shallow karst soils (Zhang 2017; Bi *et al.* 2024; Georgiou *et al.* 2022). In August 2023, three vegetation types were investigated: grassland (G), arboreal forest (A), and shrubland (S). For each vegetation type, three replicate plots were established with distances > 500 m between plots. Within each plot, nine subplots (20 m × 20 m) were arranged in a grid pattern. Composite soil samples (0–20 cm) were collected using a W-pattern sampling strategy. Each sample was divided into two portions: one stored at −80° C for microbial analysis and the other air-dried for physicochemical analysis. Soil physicochemical properties were determined following standard procedures (Bi *et al.* 2024). Soil organic carbon was measured using potassium dichromate oxidation, and soil pH was determined at a water-to-soil ratio of 2.5:1. Soil texture was analyzed using the pipette method. The MAOC fraction (< 53 μm) was isolated following established procedures (Li *et al.* 2024b; Li *et al.* 2025b). Briefly, air-dried soil was dispersed using sodium hexametaphosphate, sieved at 53 μm, and the fine fraction was dried and analyzed for organic carbon content.

Microbial community analysis

High-throughput sequencing of bacterial 16S rRNA genes and fungal ITS regions was conducted using the Illumina PE300 platform (Majorbio Bio-Pharm Technology Co., Ltd.). DNA was extracted using the FastDNA® Spin Kit for Soil and checked by agarose gel electrophoresis. The V3–V4 region of bacterial 16S

EQA 75 (2026): 62 - 73

DOI: 10.60923/issn.2281-4485/25018

Table 1 . *Distribution of sampling plots and vegetation types in the study area*

Plot ID	Vegetation Type	Location	Geographic Coordinates (E, N)	Dominant Plant Species	Habitat Conditions
G1	Grassland	Chaixinzhai	105°45'40.20" E，26°21'31.39" N 105°45'40.22" E，26°21'30.71" N 105°45'40.30" E，26°21'30.25" N	*Rosa rugosa* Thunb., *Bidens pilosa* L., *Alternanthera philoxeroides* (Mart.) Griseb., *Crassocephalum crepidioidesc* (Benth.) S. Moore, *Imperata cylindrica* (L.) P. Beauv.	Transition stage of grassland restoration after cropland abandonment; vegetation coverage >80%
G2	Grassland	Xinzhai	105°46'59.71" E，26°15'23.89" N 105°46'59.45" E，26°15'23.84" N 105°46'59.60" E，26°15'23.57" N		Low herbaceous community;shallow soil layer
G3	Grassland	Xiaba	105°46'38.56" E，26°15'02.01" N 105°46'38.28" E，26°15'01.69" N 105°46'37.84" E，26°15'01.37" N		Adjacent to bedrock-exposed areas
A1	arboreal forest	Chaixinzhai	105°45'40.65" E，26°21'32.54" N 105°45'41.54" E，26°21'32.12" N 105°45'41.70" E，26°21'32.85" N	*Cunninghamia lanceolata* (Lamb.) Hook., *Platycladus orientalis* (L.) Franco, *Prunus cerasifera 'Atropurpurea'* *Euonymus hamiltonianus* Wall.	Deciduous-evergreen mixed forest;high canopy density
A2	arboreal forest	Chaixinzhai	105°45'52.00" E，26°21'27.32" N 105°45'50.77" E，26°21'28.08" N 105°45'51.37" E，26°21'27.87" N		Deciduous-evergreen mixed forest;high canopy density
A3	arboreal forest	Zhaojiatian、Xinzhai	105°47'14.67" E，26°16'7.49" N 105°47'15.07" E，26°16'6.71" N 105°47'15.55" E，26°16'5.72" N		Steep terrain; calcium-rich soil
S1	Shrubland	Longga	105°45'21.23" E，26°22'12.22" N 105°45'21.33" E，26°22'12.03" N 105°45'20.97" E，26°22'12.14" N	*Coriaria nepalensis* Wall.c、*Arundo donax* L.、*Berchemia sinica* C. K. Schneid.、*Itea yunnanensis* Franch.	Dense shrub thicket;plant height 1.5–3 m
S2	Shrubland	Xinzhai	105°47'03.39" E，26°15'43.15" N 105°47'03.33" E，26°15'42.80" N 105°47'02.99" E，26°15'42.60" N		Minimal human disturbance;high organic matter input
S3	Shrubland	Xinzhai	105°46'58.86" E，26°15'24.16" N 105°46'58.86" E，26°15'24.76" N 105°46'58.45" E，26°15'23.72" N		Dense shrub thicket;plant height 1.5–3 m

Note: G, A, and S represent grassland, arboreal forest, and shrubland, respectively. Plot IDs indicate replicate plots within each vegetation type.

rRNA genes was amplified using primers 338F/806R, and fungal ITS regions were amplified using ITS1F/ITS2R primers. PCR products were purified, quantified, and used for library construction. Operational taxonomic units (OTUs) were clustered at 97% similarity using UPARSE v7.1. Low-abundance OTUs and non-target sequences (e.g., chloroplasts and mitochondria) were removed to improve data quality. Taxonomic annotation was performed using the SILVA database (release 138) for bacteria and the UNITE database (release 8.0) for fungi.

Data processing and statistical analysis

ASTER GDEM data (30 m resolution) were used to characterize topographic features, and spatial maps were generated using ArcGIS 10.8. Microbial alpha diversity was evaluated using the Chao1 (richness), Shannon (diversity), and Coverage indices, calculated in mothur (v1.30.2). Beta diversity was assessed using non-metric multidimensional scaling (NMDS) based on Bray–Curtis distances in QIIME2, with visualization performed in R using the vegan package. To evaluate relationships among soil properties, microbial communities, and carbon fractions, structural equation modeling (SEM) was conducted. Observed variables were grouped into composite factors to reduce model complexity, including soil physical properties, soil chemical properties, bacterial traits, and fungal traits. The fungal-to-bacterial ratio (F/B) was included as an explanatory variable. Distance-based redundancy ana-

EQA 75 (2026): 62 - 73

DOI: 10.60923/issn.2281-4485/25018

lysis (db-RDA) was performed to assess associations between environmental variables and microbial community composition. Other statistical analyses were conducted using SPSS 27.0, Origin 2022, and Excel 2010. Statistical significance was determined at $P < 0.05$.

Results

Distribution of MAOC and soil physicochemical properties across vegetation types

MAOC content differed among vegetation types, following the order arboreal forest (5.54 g/kg) > shrubland (2.83 g/kg) > grassland (1.84 g/kg) (Fig. 2). Arboreal forest soils had significantly higher MAOC content than grassland soils ($P < 0.01$), whereas differences between arboreal forest and shrubland and between shrubland and grassland were not significant. The variability of MAOC was greater in arboreal forest soils than in grassland soils ($P < 0.01$). SOC content followed the order shrubland (39.72 g/kg) > arboreal forest (36.48 g/kg) > grassland (28.30 g/kg). The MAOC/SOC ratio decreased from arboreal forest (15.78%) to shrubland (9.76%) and grassland (7.97%), with a regional mean of 12.22% (Fig. 2). Significant within-group variability in MAOC was observed in arboreal forest and grassland, whereas shrubland showed no significant intragroup variation (Fig. 2).

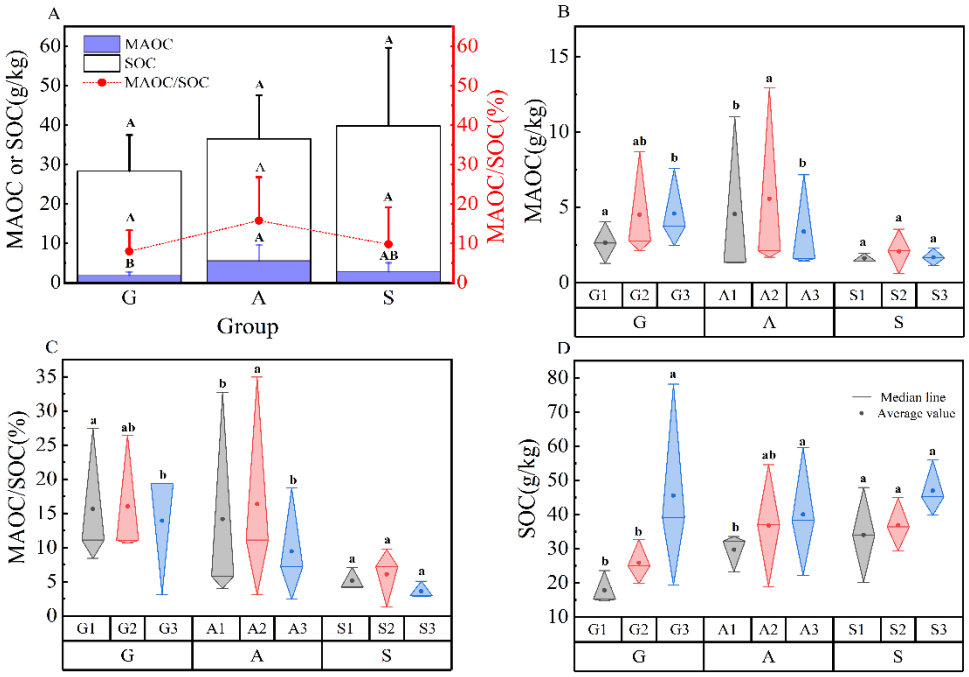

Figure 2
Differences in MAOC content and MAOC/SOC ratio among vegetation types. Note: MAOC, mineral-associated organic carbon; SOC, soil organic carbon. G, A, and S represent grassland, arboreal forest, and shrubland, respectively. Different uppercase letters indicate significant differences among vegetation types ($P < 0.05$), while different lowercase letters indicate significant differences within the same vegetation type ($P < 0.05$).

Soil texture differed significantly among vegetation types (Fig. 3). Arboreal forest soils had the highest sand content (50.33%), significantly higher than that of grassland soils (29.44%; $P < 0.05$). Grassland soils had the highest clay content (34.07%), exceeding that of arboreal forest (16.27%) and shrubland (23.71%). By contrast, no significant differences were observed in major soil chemical properties among vegetation types (Fig. 4). Total nitrogen (TN) and total phosphorus (TP) were highest in arboreal forest soils (3.43 g/kg and 0.65 g/kg, respectively), while shrubland soils had the lowest TP (0.56 g/kg). Soil pH ranged from 7.39 to 7.67, indicating generally neutral to weakly alkaline conditions across all vegetation types. Stoichiometric ratios (C/N, C/P, N/P) varied among vegetation types, with higher values observed in shrubland and arboreal forest

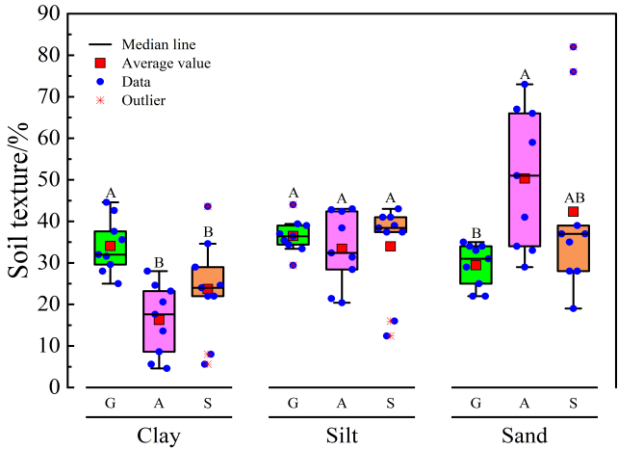

Figure 3. *Soil texture composition among vegetation types. Note: G, A, and S represent grassland, arboreal forest, and shrubland, respectively. Different uppercase letters indicate significant differences among vegetation types ($P < 0.05$).*

EQA 75 (2026): 62 - 73

DOI: 10.60923/issn.2281-4485/25018

forest compared with grassland (Figs. 3, 8a).

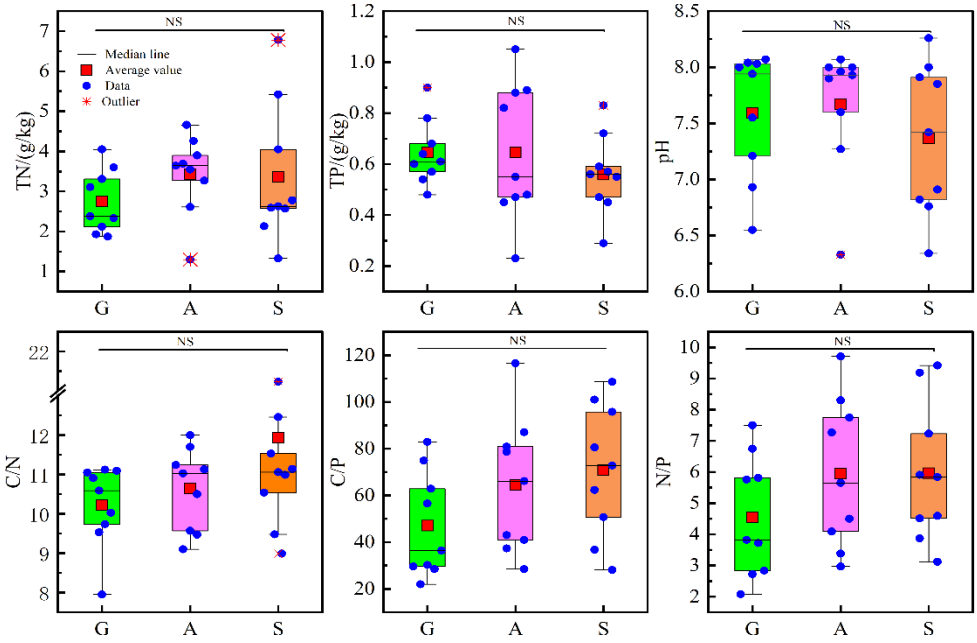

Figure 4
Differences in soil environmental factors among vegetation types. Note: SOC, soil organic carbon; TN, total nitrogen; TP, total phosphorus; C/N, carbon-to-nitrogen ratio; C/P, carbon-to-phosphorus ratio; N/P, nitrogen-to-phosphorus ratio; NS, no significant difference among vegetation types. G, A, and S represent grassland, arboreal forest, and shrubland, respectively.0

Microbial community characteristics across vegetation types

No significant differences were observed in bacterial or fungal Chao1 and Shannon indices among vegetation types ($P > 0.05$). However, shrubland showed the highest bacterial and fungal richness, while grassland and arboreal forest showed the highest bacterial and fungal diversity indices, respectively (Table 2). Bacterial richness and diversity were consistently higher than fungal richness and diversity across all vegetation types. Intragroup variability was observed in grassland and arboreal forest ($P < 0.05$), while shrubland showed relatively lower variability (Table 2). Dominant bacterial phyla across all vegetation types included Proteobacteria, Acidobacteriota, and Actinobacteriota (Fig. 5). Actinobacteriota had the highest relative abundance in grassland (17.54%), Acidobacteriota dominated arboreal forest (22.85%), and Proteobacteria were most a-

Table 2. *Diversity Indexes of soil microorganisms.*

Group	Bacteria Chao1 index	Bacteria Shannon index	Fungi Chao1 index	Fungi Shannon index
G	4287.3±353.8A	6.721±0.330A	766.365±135.001A	4.413±0.594A
A	4329.1±285.8A	6.714±0.161A	758.443±200.304A	4.759±0.319A
S	4503.2±442.0A	6.698±0.314A	890.287±30.5591A	4.296±1.200A

Note: G, A, and S represent grassland, arboreal forest, and shrubland, respectively. Chao1 and Shannon indices represent microbial richness and diversity, respectively. Values are means ± standard deviations. Different uppercase letters in the same column indicate significant differences among vegetation types ($P < 0.05$). Intragroup variations are described in the main text.

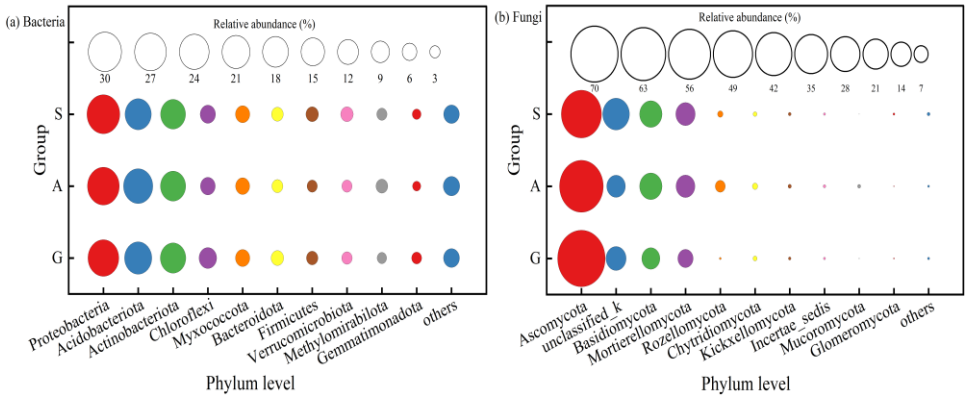

Figure 5
Composition of soil bacterial and fungal communities at the phylum level. Note: G, A, and S represent grassland, arboreal forest, and shrubland, respectively. Relative abundance indicates the percentage of each bacterial or fungal phylum in the corresponding microbial community.

DOI: 10.60923/issn.2281-4485/25018

bundant in shrubland (29.02%). Fungal communities were dominated by Ascomycota across all vegetation types, with higher abundance in grassland (68.78%) compared with shrubland (58.12%) and arboreal forest (62.15%). Arboreal forest also showed relatively higher abundances of Basidiomycota and Rozellomycota (Fig. 5). NMDS analysis (Stress < 0.2) indicated differences in microbial community composition among vegetation types (Fig. 6). Bacterial communities showed partial overlap between arboreal forest and shrubland, whereas fungal communities exhibited greater dispersion within groups. ANOSIM analysis showed significant differences in fungal communities between arboreal forest and shrubland ($P < 0.05$), while bacterial differences were less pronounced.

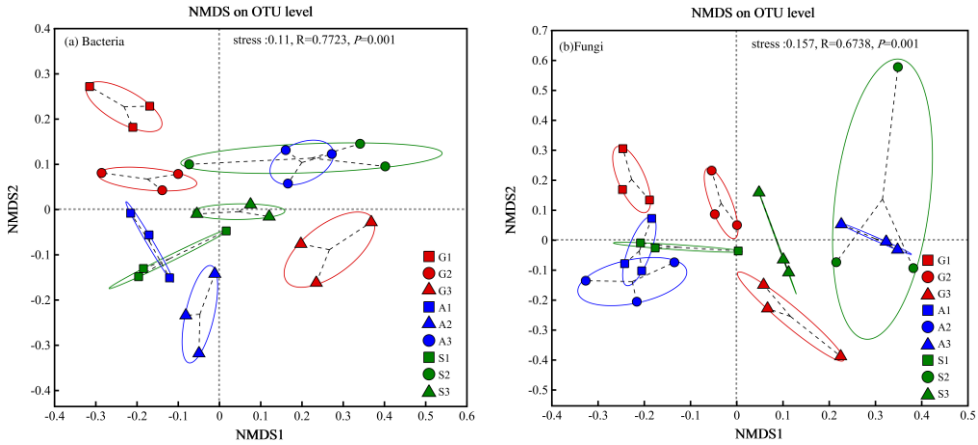

Figure 6
NMDS analysis of soil microbial communities at the OTU level. Note: NMDS, non-metric multidimensional scaling; OTU, operational taxonomic unit. G, A, and S represent grassland, arboreal forest, and shrubland, respectively. Points represent soil samples, and shorter distances between points indicate greater similarity in microbial community composition.

Associations of soil factors and microbial communities with MAOC

Distance-based redundancy analysis (db-RDA) showed that microbial taxa differed in their relationships with MAOC (Fig. 7). Actinobacteriota and Acidobacteriota were positively associated with MAOC, whereas Proteobacteria showed a negative association. In fungal communities, Ascomycota was positively associated with MAOC, while Basidiomycota and unclassified fungi were negatively associated and more closely related to clay and silt fractions. Correlation analysis showed that MAOC was positively associated with Actinobacteriota abundance, soil pH, and sand content, (Fig. 8a). The MAOC/SOC ratio showed similar asso-

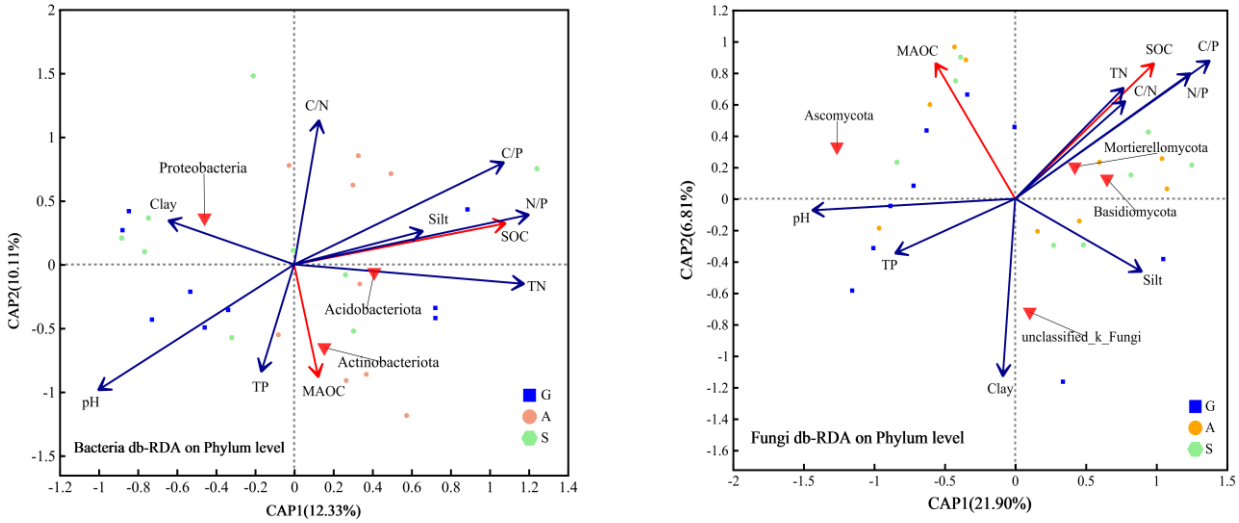

Figure 7. *Distance-based redundancy analysis of environmental factors, microbial community, and samples. Note: Dots of different colors and shapes represent samples in different environments or conditions; The length of the arrow represents the degree of influence of environmental factors on microorganisms and samples; The angle between the arrows is positively correlated, the obtuse angle is negatively correlated, and the right angle is no correlation. The distance from the projection point from the sample point to the arrow point and the origin point represents the relative influence of environmental factors on the sample and microbial distribution, the direction of the point and the arrow is consistent for positive correlation, and the direction of the opposite direction represents negative correlation.*

EQA 75 (2026): 62 - 73

DOI: 10.60923/issn.2281-4485/25018

ciations with microbial and soil variables. Vegetation-specific patterns were observed. In grassland soils, MAOC was negatively associated with TN and C/P, while the MAOC/SOC ratio was positi- vely associated with Ascomycota and pH (Fig. 8b). In arboreal forest soils, MAOC was positively associated with sand content and Actinobacteriota, and negatively associated with clay content and the F/B ratio (Fig. 8c). In shrubland soils, sand content was positively associated with MAOC, whereas clay and TP showed negative associations (Fig. 8d).

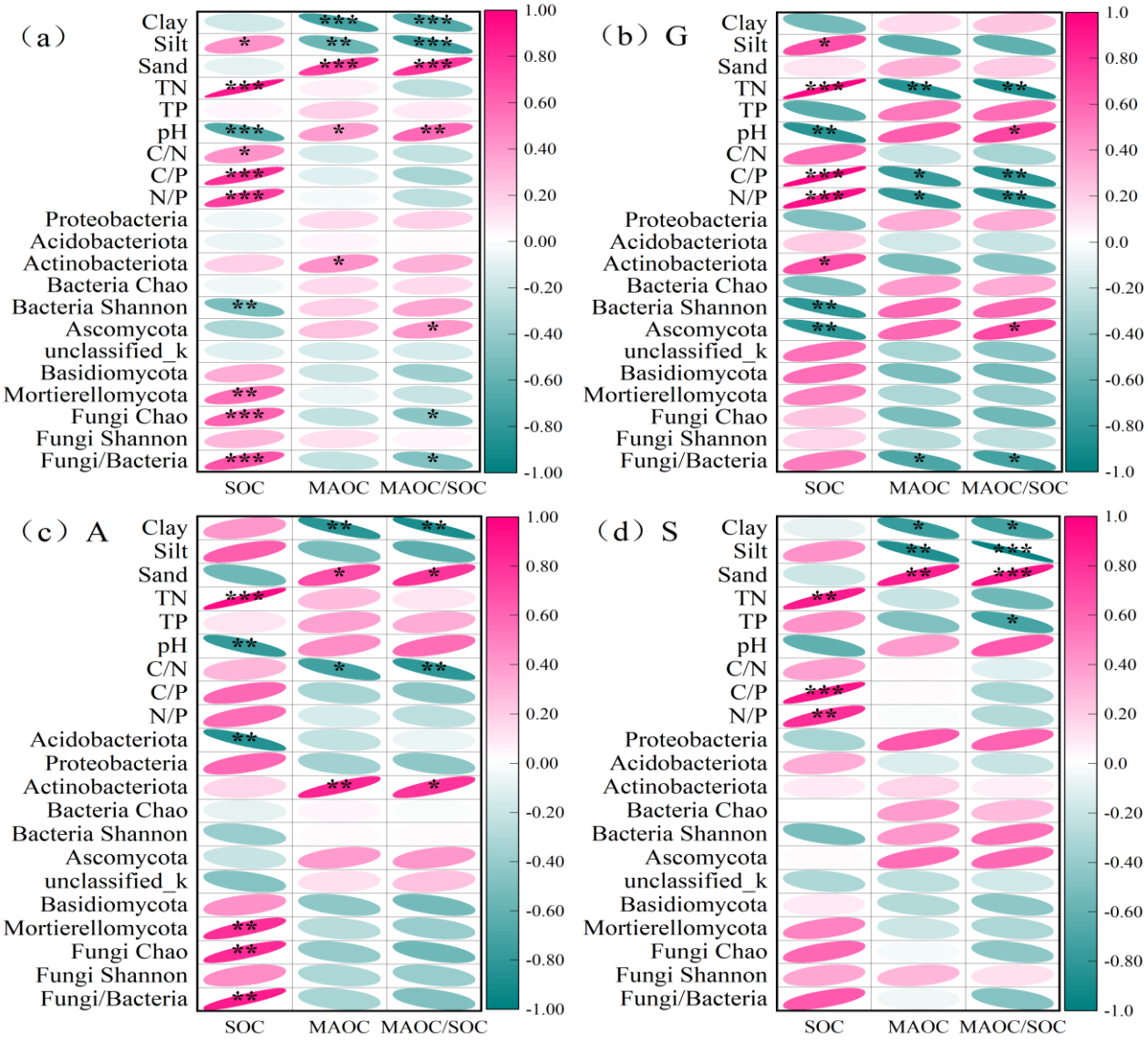

Figure 8. *Spearman's rank correlation analysis of soil MAOC with environmental and microbial factors across vegetation types. Note: Red indicates positive correlations, dark green denotes negative correlations, with color intensity reflecting correlation strength:(a) Entire study area;(b) Grassland soils;(c) Arboreal forest soils;(d) Shrubland soils.*

Structural equation modeling (SEM) showed that soil physicochemical properties were associated with MAOC both directly and indirectly through microbial variables (Fig. 9; Table 3). Soil physical properties showed a negative direct association with MAOC ($\beta = -0.82$), while soil chemical properties showed a weaker negative direct association ($\beta = -0.26$). Soil chemical properties were positively associated with fungal traits and the fungal-to-bacterial ratio. The model explained 77% of the variation in MAOC. Overall, variation in MAOC among vegetation types was associated with composition, whereas soil chemical properties showed relatively limited variation. the differences in soil texture and microbial community composition, whereas soil chemical properties showed relatively limited variation.

EQA 75 (2026): 62 - 73

DOI: 10.60923/issn.2281-4485/25018

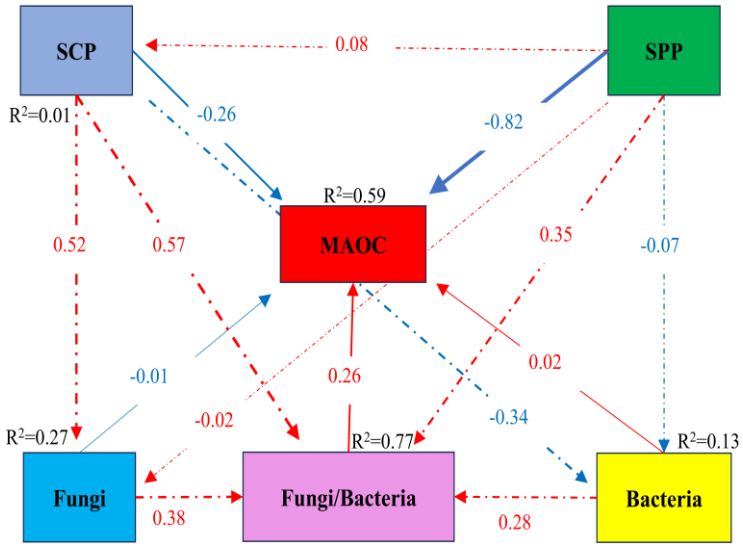

Figure 9

Structural equation model (SEM) illustrating interactive drivers of MAOC formation via soil physicochemical-mineral protection and microbial processes. SEM Legend: ①Pathways: Red arrows = positive effects (β > 0), blue arrows = negative effects (β < 0). Line thickness scales with absolute path coefficients (thin: |β| ≤ 0.1; medium: 0.1 < |β| < 0.3; thick: |β| ≥ 0.3). ②Line Types: Solid lines = direct factors affecting MAOC; dashed lines = interactions between soil physicochemical-mineral protection and microbial variables. ③Variables: Exogenous variables (SPP: pink box; SCP: blue box), endogenous variables (MAOC: gray box; Fungi, Bacteria, F/B). Path coefficients labeled adjacent to arrows; R² values listed within variable boxes. ④Significance: Thick-line paths are significant by default (P< 0.05).

Table 3. *Structural Equation Model Fit Indices*

Indicator	Value	Benchmark	Interpretation
χ^2	0.645	-	Chi-square statistic
df	1.000	-	Degrees of freedom
p-value	0.422	> 0.05 (non-significant)	No significant model-data discrepancy
CFI	1.000	> 0.95 (excellent)	Comparative Fit Index
NFI	0.992	> 0.95 (excellent)	Normed Fit Index
IFI	1.005	> 0.95 (excellent)	Incremental Fit Index
RMSEA	0.000	< 0.06 (excellent)	Root Mean Square Error of Approximation
AIC	342.684	Lower values preferred	Akaike Information Criterion
BIC	367.305	Lower values preferred	Bayesian Information Criterion

Note: χ^2, chi-square statistic; df, degrees of freedom; CFI, comparative fit index; NFI, normed fit index; IFI, incremental fit index; RMSEA, root mean square error of approximation; AIC, Akaike information criterion; BIC, Bayesian information criterion. The p-value indicates whether there is a significant discrepancy between the model and the observed data. Lower AIC and BIC values indicate better relative model fit when comparing alternative models.

Discussion

Low MAOC amount despite potential mineral protection in karst soils

This study showed that the proportion of MAOC in karst soils (regional mean MAOC/SOC ratio: 12.22%) was relatively low compared with many ecosystems reported in the literature, despite environmental conditions that may favor mineral protection. Across other ecosystems, MAOC accounts for a large proportion of SOC, but exhibits strong variability depending on ecosystem type and environmental conditions (Lv *et al.* 2023; Li *et al.* 2024a). In karst systems, such variability may be related to the combined effects of shallow soils, discontinuous substrates, rapid drainage, and Ca^{2+}-rich geochemical

EQA 75 (2026): 62 - 73

DOI: 10.60923/issn.2281-4485/25018

conditions (Bi *et al.* 2024; Sokol *et al.* 2022; Huang *et al.* 2021). These characteristics are consistent with a system in which mineral protection processes may occur, while net MAOC amount remains relatively limited. In the present study, MAOC content in arboreal forest soils was higher than that in grassland soils, but still lower than values reported for many temperate forest ecosystems (Sokol *et al.* 2022). This pattern may reflect differences in litter input, microbial processing, and environmental constraints such as nutrient availability and drainage conditions (Zhu *et al.* 2024; Underwood *et al.* 2024). Rapid drainage and shallow soil depth may reduce substrate retention and increase carbon loss, thereby limiting the accumulation of mineral-associated carbon even under conditions favorable to Ca-mediated stabilization (Bi *et al.* 2024; Huang *et al.* 2021). Overall, these results suggest that karst soils may exhibit relatively strong mineral protection potential but comparatively low MAOC amount.

Association between MAOC and soil texture in karst soils

A notable result of this study was the negative association between MAOC and clay content. In many non-karst systems, clay minerals provide reactive surfaces that enhance organic carbon stabilization (Sokol *et al.* 2022). In the present study, however, this relationship differed from the conventional pattern. Such differences may be related to carbonate-dominated geochemistry and high Ca^{2+} availability in karst soils. Under these conditions, Ca-mediated interactions and organo-mineral co-precipitation may play an important role in carbon stabilization (Huang *et al.* 2021; Li *et al.* 2025a). Grassland soils had the highest clay content but the lowest MAOC, whereas arboreal forest soils showed lower clay content and higher MAOC. In addition, MAOC was positively associated with sand content. These patterns suggest that soil texture alone may not fully explain MAOC variation in karst soils and that alternative stabilization pathways may be involved. High clay content may also be associated with reduced aeration or changes in microhabitat conditions, which could influence microbial processing and carbon transformation (Li *et al.* 2025b). Overall, MAOC stabilization in karst soils appears to be influenced by multiple interacting factors, including mineral composition, Ca availability, and microbial activity.

Role of vegetation and microbial communities in MAOC variation

The relatively low MAOC content in grassland soils suggests that vegetation type and possible land-use history may influence carbon stabilization. Previous studies have shown that disturbance can reduce the conversion of organic matter into mineral-associated fractions (Begill *et al.* 2023; Li *et al.* 2024b). Although land-use history was not directly quantified in this study, the observed differences between vegetation types are consistent with the possibility that past disturbance and current vegetation jointly influence MAOC distribution. Microbial results further indicate that MAOC variation was more closely related to community composition than to overall diversity. The positive associations of Actinobacteriota and Ascomycota with MAOC suggest that specific microbial groups may contribute to residue formation and mineral interactions (Liang *et al.* 2023). Vegetation-type differences in nutrient stoichiometry may also influence microbial activity and residue stabilization. These findings are consistent with a coupled interaction among soil properties, microbial communities, and vegetation in regulating MAOC dynamics.

Implications for ecosystem management and future research

From a management perspective, the results indicate that vegetation type may influence carbon stabilization potential in karst soils. Arboreal forest soils showed relatively higher MAOC levels, whereas grassland and shrubland soils were associated with lower MAOC values. These patterns highlight the importance of considering vegetation–soil–microbe interactions when evaluating soil quality and carbon storage in karst ecosystems. However, the present study is based on observational data, and causal relationships cannot be fully established. Future research should focus on experimental approaches to evaluate MAOC formation processes, including microbial residue stabilization, mineral interactions, and nutrient limitations. Long-term monitoring across vegetation types would also help clarify the mechanisms controlling carbon stabilization in heterogeneous karst landscapes. This study is based on observational data; therefore, results reflect associations rather than causal relationships.

Conclusions

This study showed that MAOC in limestone-derived

DOI: 10.60923/issn.2281-4485/25018

karst soils varied among vegetation types and was associated with microbial community composition and soil physicochemical properties. Arboreal forest soils had the highest MAOC content, followed by shrubland and grassland. Across the study area, MAOC was positively associated with Actinobacteriota abundance, soil pH, and sand content, but negatively associated with clay and silt contents. These results suggest that MAOC dynamics in karst soils are linked to vegetation type, soil texture, microbial community structure, and carbonate-related soil conditions. Because this study was observational, further experimental work is needed to clarify the mechanisms controlling MAOC formation and persistence, particularly the roles of microbial residues, mineral interactions, Ca-mediated stabilization, and nutrient availability.

Acknowledgements

The authors thank all colleagues and field assistants who supported sample collection and laboratory analysis.

Disclosure statement

No potential conflict of interest was reported by the author(s).

Funding

This work was supported by the Guizhou Provincial Basic Research Program (Natural Science) (No. MS[2025]326), the Guizhou Provincial Key Technology R&D Program (No. QKHZC [2023] 204 and QKHZC [2023] 141), the Science and Technology Projects of Guizhou Province (No. QKHPT-YWZ[2024]005), and the Talent Team Project of Guizhou Institute of Biology (No. QSS2024001).

References

ANGST G., MUELLER K.E., NIEROP K.G.J., SIMPSON M.J. (2021) Plant or microbial-derived? A review on the molecular composition of stabilized soil organic matter. Soil Biology and Biochemistry, 156: 108189. https://doi.org/10.1016/j.soilbio.2021.108189

BEGILL N., DON A., POEPLAU C. (2023) No detectable upper limit of mineral-associated organic carbon in temperate agricultural soils. Global Change Biology, 29: 4662–4669. https://doi.org/10.1111/gcb.16804

BI X., YAO Y., WANG Z.C., LI C.H., CAO D., WEN L.W., JING L., SUN B.F. (2024) Improving monitoring karst rocky desertification using high-frequency Landsat observations: A generalized framework and its application, to a typical karst region in southeast China. CATENA, 241: 108045. https://doi.org/10.1016/j.catena.2024.108045

DAI B., PENG T., ZHANG X.B., MO X.M., WANG S.J. (2023) Major types and formation mechanism of karst hills in plateau and discussion on karst landform zoning in Guizhou, China. Mountain Research, 41: 155–168. https://doi.org/10.16089/j.cnki.1008-2786.000738

GEORGIOU K., JACKSON R.B., VINDUŠKOVÁ O., ABRAMOFF R.Z., AHLSTRÖM A., FENG W., HARDEN J.W., PELLEGRINI A.F.A., POLLEY H.W., SOONG J.L., RILEY W.J., TORN M.S. (2022) Global stocks and capacity of mineral-associated soil organic carbon. Nature Communications, 13: 3797. https://doi.org/10.1038/s41467-022-31540-9

GEORGIOU K., KOVEN C.D., WIEDER W.R., HARTMAN M.D., RILEY W.J., PETT-RIDGE J., BOUSKILL N.J., ABRAMOFF R.Z., SLESSAREV E.W., AHLSTRÖM A., PARTON W.J., PELLEGRINI A.F.A., PIERSON D., SULMAN B.N., ZHU Q., JACKSON R.B. (2024) Emergent temperature sensitivity of soil organic carbon driven by mineral associations. Nature Geoscience, 17:205–212. https://doi.org/10.1038/s41561-024-01384-7

HE J., LIU X., MENG W., CHEN X. (2024) Recent advances in studies of soil organic carbon stability in Karst areas. Frontiers in Forests and Global Change, 7: 1453615. https://doi.org/10.3389/ffgc.2024.1453615

HU P., ZHANG W., NOTTINGHAM A.T., XIAO D., KUZYAKOV Y., XU L., CHEN H., XIAO J., DUAN P., TANG T., ZHAO J., WANG K. (2024). Lithological controls on soil aggregates and minerals regulate microbial carbon use efficiency and necromass stability. Environmental Science and Technology, 58: 21186–21199. https://doi.org/10.1021/acs.est.4c07264

HUANG J.S., LIU W.X., YANG S., YANG L., PENG Z.H., DENG M.F., XU S., ZHANG B., AHMAD I., YANG Y.H., LIU L.L. (2021). Plant carbon inputs through shoot, root, and mycorrhizal pathways affect soil organic carbon turnover differently. Soil Biology and Biochemistry, 160: 108322. https://doi.org/10.1016/j.soilbio.2021.108322

LI J.N., CHEN S.X., LONG X.W., HU P., XIAO D., ZHANG W., MOLDOVAN O.T., ZHAO J., WANG K.. (2025a). Linking rock outcrop size and distance to soil multifunctionality in mountain ecosystems. Functional Ecology, 39: 1288–1301. https://doi.org/10.1111/1365-2435.70034

LI W.D., CHEN D., CHENG J.L., FANG Q.L., HU L.X., WANG T.Y., LI C.J., ZHAO B., LI Q.Q. (2025b) Characteristics and influencing factors of soil particulate and mineral-associated organic carbon in cropland soil across Sichuan basin. Environmental Science, 46: 388–398. https://doi.org/10.13227/j.hjkx.202402001

DOI: 10.60923/issn.2281-4485/25018

LI Y., FENG X., WU L.H., LUO G.J., LUO H.F. (2024a) Spatial-temporal evolution and quantitative attribution of habitat quality in typical karst counties of Guizhou plateau. Environmental Science, 45: 2793–2805. https://doi.org/10.13227/j.hjkx.202306238

LI Z., DUAN X., GUO X.B., GAO W., LI Y., ZHOU P., ZHU Q.H., O'DONNEL A.G., DAI K., WU J.S.. (2024b). Microbial metabolic capacity regulates the accrual of mineral-associated organic carbon in subtropical paddy soils. Soil Biology and Biochemistry, 195: 109457. https://doi.org/10.1016/j.soilbio.2024.109457

LIANG G.P., STARK J., WARING B.G. (2023). Mineral reactivity determines root effects on soil organic carbon. Nature Communications, 14: 4962. https://doi.org/10.1038/s41467-023-40768-y

LIAO J.J., YANG X., DOU Y.X., WANG B.R., XUE Z.J., SUN H., YANG Y., AN S.S.. (2023). Divergent contribution of particulate and mineral-associated organic matter to soil carbon in grassland. Journal of Environmental Management, 344:118536. https://doi.org/10.1016/j.jenvman.2023.118536

LV J.F., SHI J., WANG Z., PENG Y.M., WANG X. (2023). Effects of erosion and deposition on the extent and characteristics of organic carbon associated with soil mineral in Mollisol landscape. CATENA, 228: 107190. https://doi.org/10.1016/j.catena.2023.107190

SOKOL N.W., WHALEN E.D., JILLING A., KALLENBACH C.M., GEORGIOU K. (2022) Global distribution, formation and fate of mineral-associated soil organic matter under a changing climate: A trait-based perspective. Functional Ecology, 36: 1411–1429. https://doi.org/10.1111/1365-2435.14040

SONG W.J., LIANG Y.Z., TAO Z., ZHONG Q.X., HE Y.C. (2023) Advances on soil organic carbon dynamics mediated by microorganisms. Advances in Earth Science, 38: 1213–1223. https://doi.org/10.11867/j.issn.1001-8166.2023.076

SU X., QU C., KANG J., GAO D., CAI P., CHEN W., HUANG Q. (2024) Microorganisms drive mineral-associated organic carbon formation. Science Bulletin, 69: 3327–3338. https://doi.org/10.1360/TB-2023-1049

TONG Y., XIANG H.Q., JIANG J., CHEN W. (2024) Interfacial interactions between minerals and organic matter: Mechanisms and characterizations. Chemosphere, 359: 142383. https://doi.org/10.1016/j.chemosphere.2024.142383

UNDERWOOD T.R., BOURG I.C., ROSSO K.M. (2024) Mineral-associated organic matter is heterogeneous and structured by hydrophobic, charged, and polar interactions. Proceedings of the National Academy of Sciences of the United States of America, 121: e2413216121. https://doi.org/10.1073/pnas.2413216121

WU H.W., CUI H.L., FU C.X., LI R., QI F.Y., LIU Z.L., YANG G., XIAO K.Q.(2024) Unveiling the crucial role of soil microorganisms in carbon cycling: A review. Science of the Total Environment, 909: 168627. https://doi.org/10.1016/j.scitotenv.2023.168627

WU M.Y., CHEN L., CHEN S.G., CHEN Y.L., MA J.P., ZHANG Y.Q., PANG D.B., LI X.B. (2025) Soil microbial carbon and nitrogen limitation constraints soil organic carbon stability in arid and semi-arid grasslands. Journal of Environmental Management, 373: 123675. https://doi.org/10.1016/j.jenvman.2024.123675

XIAO L.Y., WU X.Q., GUO C.Q., LU Z.C., KHAN M.A., ZHENG C.H., ZHOU J.X. (2025) Thriving amidst adversity.Responses of karst vegetation to extreme compound droughts. Journal of Hydrology, 659: 133216. https://doi.org/10.1016/j.jhydrol.2025.133216

ZHANG Z.M. (2017). Soil organic carbon distribution and vegetation restoration in karst areas. PhD thesis, Guizhou University.

ZHOU Z.H., REN C.J., WANG C.K., DELGADO-BAQUERIZO M., LUO Y.Q., LUO Z.K., DU Z.G., ZHU B., YANG Y.H., JIAO S., ZHAO E.Z., CAI A.D., YANG G.H., WEI G.H. (2024) Global turnover of soil mineral associated and particulate organic carbon. Nature Communications, 15: 5329. https://doi.org/10.1038/s41467-024-49743-7

ZHU E.X., LIU Z.G., MA L.X., LUO J.N., KANG E.Z., WANG Y., ZHAO Y.P., JIA J., FENG X.J. (2024) Enhanced mineral preservation rather than microbial residue production dictates the accrual of mineral-associated organic carbon along a weathering gradient. . Geophysical Research Letters, 51: e2024GL108466. https://doi.org/10.1029/2024GL108466